Fuel 264 (2020) 116806

Contents lists available at ScienceDirect

Fuel

journal homepage: www.elsevier.com/locate/fuel

Full Length Article

Experimental study of smouldering in wood pellets with and without air draft

Virginia Rebaque[a], Ivar S. Ertesvåg[a,*], Ragni Fjellgaard Mikalsen[b,c,d], Anne Steen-Hansen[b]

[a] Department of Energy and Process Engineering, NTNU Norwegian University of Science and Technology, NO-7491 Trondheim, Norway
[b] RISE Fire Research, Trondheim, Tillerbruvegen 202, NO-7092 Tiller, Norway
[c] Western Norway University of Applied Sciences, Bjørnsonsgate 45, NO-5528 Haugesund, Norway
[d] Otto von Guericke University Magdeburg, Universitätsplatz 2, DE-39106 Magdeburg, Germany

ARTICLE INFO

Keywords:
Smolder
Fire
Combustion
Poros media
Buoyancy
Internal air motion

ABSTRACT

Dry wood pellets (diameter 8 mm) of mixed Norwegian spruce and pine were tested in samples of 1.25 kg (1.7 l) in configurations with and without air draft from below. The pellets were placed in a vertical 15 cm diameter cylinder on top of a hot plate. Air draft inlet, when allowed, came through narrow openings in the cylinder bottom periphery. The bulk void of 36% formed channels for gas flows within the pellets bed. Initially, the samples were heated externally from below for 6 h. Time series of distributed temperatures were recorded, together with values of the mass. Smouldering with air draft was observed with two distinct behaviours: Type 1, where the sample after the period of external heating cooled down for several hours, and then increased in temperature to intense smouldering, and Type 2, where the sample went into intense smouldering before the end of external heating. Without draft airflow from below, the sample cooled down after external heating, before developing into intense smouldering about 20 h later. In all cases, the intense period lasted for 2 h. Typical temperatures were in the range 300–450 °C, while higher temperatures occurred in the intense period. Draft flow caused fast oxidation spreading, while slow without draft. Indications of oxidation spreading as a distriäbuted reaction were seen. Circulating air motions in the irregular void between individual pellets is discussed as an explanation for the behaviour. Uneven access to oxygen, with possibilities of locally excess air, can explain the peak temperatures observed.

1. Introduction

Smouldering is a non-flaming combustion mode. It can be harder to detect than flaming fires, occurs at lower temperatures and has a potential of releasing more of toxic gases. Smouldering derives heat from heterogeneous reactions occurring on the surface of a solid fuel when heated in an oxidizer environment [1]. The combustion process is generally oxygen deficient [2], and the propagating reaction leaves behind a char that can contain significant amounts of unburned fuel. Smouldering is of interest both as a fundamental combustion problem and as a practical fire hazard, for instance in industrial storage units and buildings.

Rein [1,3] and Ohlemiller [4] reviewed a selection of previous experimental work on smouldering, dating back to the 1950s–80s and dealing with cellulosic particles, fibres and insulation boards, cardboard, sawdust, tobacco, etc. The first of these investigators, Palmer [5], dealt with biomass dusts and fibres and metal dusts. He referred even older work (1930s) on coal dusts. In the recent few decades, experimental contributions have included work on polyurethane foams [6–9], wood and wood logs [10,11], peat [12–14], biomass or char powder [15–17], cotton [18–20], surrogate human faeces [21], bark [22,23], wood fibre insulation [24] and cellulose/hemicellulose with different densities [25].

Effects of gravity were investigated experimentally by Dosanjh et al. [26] for porous cellulose (83% void), and Torero and Fernandez-Pello [27,6] for polyurethane (97.5% void), while explored numerically by Lutsenko and Levin [28]. These investigations revealed that complex flows could be set up in porous materials due to buoyancy. Bar-Ilan et al. [8,9] showed that buoyant flows were important for smouldering, as they had a great influence on heat transfer and on key species mass transfer.

Simply explained, smouldering differs from flaming in that oxidation and heat release occur on the solid surface of the fuel. Flaming combustion is commonly regarded as visible, gas-phase reactions

* Corresponding author.
E-mail address: ivar.s.ertesvag@ntnu.no (I.S. Ertesvåg).

https://doi.org/10.1016/j.fuel.2019.116806
Received 3 July 2019; Received in revised form 27 November 2019; Accepted 30 November 2019

adjacent to or surrounding the solid fuel. There is also a difference in the range of temperatures; maximum temperatures in smouldering combustion are typically found around 500–700 °C [3], although both higher and lower levels are reported in some experiments. The higher temperatures may be attributed to char oxidation [29]. In comparison, flaming combustion of solid fuels can show much higher maximum temperatures.

Smouldering propagation appears to be controlled by two factors: oxygen availability to the smouldering front and the heat transfer to or from it [2]. When external heating is prolonged in time, an assisted propagation is possible. If the external heat supply ceases, the smouldering will be either self-sustained or extinct. Smouldering is commonly classified into two different configurations: opposed (aka. reverse) and forward [30,31,1], according to the direction of the oxygen flow relative to the smouldering direction. However, except in very simple configurations, a real case may over time and space comprise both directions.

In transition from smouldering to flaming, gas-phase reactions are supported by the smoulder reaction, as a source both of gaseous fuel and of the heat required to initiate the flame. According to Rein [3], transition to flaming has only been observed in forward propagation. The reason [32] is the differences in heat transfer within opposed and forward-flow configurations. Ohlemiller [32] also made a distinction between gaseous reactions within pores of the fuel, and “true” flames outside the sample. The investigations on transition to flaming are limited [31], but indicates that a combined occurrence of minimum amounts of air, pyrolysis products and thermal energy is required. Dodd et al. [33] reviewed the experimental literature, which speculated that char oxidation is a precursor to transition.

Most of the studies referred above were on materials with little or no continuous void, like solid bodies, foams and fine powder. Coarse granular materials, beds of pellets or wood chips, etc., with internal gas cavities and channels, appear to be less investigated and less understood. This includes a wide variety of substances and products of practical life, such as grain, animal fodder, fuel pellets, fertilizers. They are stored and handled by industry, agriculture, building services and home owners.

In some smouldering experiments (e.g. [15]), investigators have made care to avoid cracks in the sample (often fine grinded powder) to avoid false air flows into it. For pellets and other materials with a large void, channels for gas flows in the sample is a characteristic of the fuel. He and Behrendt [16] investigated smouldering of char granules heated from below. They observed that bigger particles (> 3 mm) required longer time and higher temperature for ignition. Experiments on a larger scale (silo > 1 m^3) were conducted by Gentilhomme et al. [34], with emphasis on the generation of combustible gases and the associated explosion potential. Work associated with the present study include Jensen [35,24] on wood-fibre building insulation materials, and Mikalsen et al. [36–39] on wood pellets.

In the present work, the material studied was biomass in the form of pellets. This fuel was chosen because there were few or no previous studies of smouldering in this material. Moreover, wood pellets are becoming widely used as an alternative to oil-fired central heating in residential and industrial buildings in Europe. It will be important to know its properties from safety reasons. The aim of this study was to investigate the smouldering behaviour in pellets by changing the airflow. Two configurations, with and without air draft from below, will be tested. The initiation will be by an external heat source under the sample, and the smouldering is expected to propagate upwards. Among the research issues is how much the air draft flow affects the intensity and propagation of smouldering, temperature level in general, its variation and peak values, depletion of mass and the elapsed time.

The article was based on the master thesis work [40,41] of the first author. The complete dataset can be found attached to the thesis at the NTNU repository.

2. Materials and method

2.1. Fuel materials

The fuel in all samples was pellets with diameter 8 mm, made of Norwegian wood. According to producer specifications, it was made of 50–80% spruce and 20–50% pine, including bark, had a unit density of 1157 kg/m^3 and a bulk density of 736 kg/m^3 (as delivered, might be slightly larger in the experiment). This gave an overall or bulk void (porosity) of 36%. The pellets were stored at low temperature at the producer’s premises for 3 months and then in a freezer in the laboratory, to avoid possible degradation (cf. [42,43]).

A sample of the fuel was analysed by Otto von Guericke University Magdeburg, Germany, using a Leco TGA701 Thermogravimetric Analyzer (www.leco.com) for the proximate analysis, a Leco CHN1000 Element Analyzer for carbon, hydrogen and nitrogen, and a Leco CS230 for Sulphur. Oxygen was evaluated as the remaining substance. The proximate analysis gave 6.27% water, 0.46% ash and 76.98% volatiles, while the ultimate analysis of the water and ash free substance gave 51.64% carbon, 3.11% hydrogen, 0.03% nitrogen, 0.11% sulphur and 42.11% oxygen. All percentages were mass based. The higher and lower heating values were determined with an IKA bomb calorimeter (www.ika.com) at, respectively, 18834 kJ/kg and 17537 kJ/kg.

2.2. Heat and mass transfer in pellets beds

Wood pellets are made by compacting sawdust at high pressure. In this process, the particles are glued together by the contained lignin. The individual pellets become dense and with a low porosity. They are fragile in the axial direction and can break up in shorter pieces, whereas in the radial direction the bindings are notably stronger. The stacking of the pellets implies that irregular channels are formed in the bed, allowing gas flows. Consequently, there are different modes of heat and mass transfer, within and between the solid pellets. Thus, the propagation of reactions fronts will also have different modes.

The heat and mass transfer of wood-pellets smouldering will have four important simultaneous subprocesses:

Convective transport and radiation in the irregular void between individual pellets.
Mass exchange into and inside the dense material of individual pellets.
Breakup and degradation of individual pellets.
Breakdown of the stacking of the bulk of pellets.

In quiescent flow, the convective transfer might be low and the drying, pyrolysis and char oxidation fronts in the pellets may be similar to more uniform materials, e.g. powder or closed-cell foams. When a buoyant draft is allowed in the channels, the reactions might be propagating from pellet to pellet by convective heat and mass transfer and gaseous reactions.

2.3. Experimental set-up

All experiments (but the fuel analysis above) were conducted in the laboratory of RISE Fire Research in Trondheim, Norway, indoor at room temperature (18–23 °C). The room was gently ventilated to maintain room air temperature and composition.

The test set-up, see Fig. 1, comprised the following parts:

In the bottom, a scale to measure the mass before, during and after the test. The scale consisted of a Kern weighing platform KFP 30V20M IP65 (www.kern-sohn.de) with a Systec IT1000 weighing terminal (www.systecnet.com).
On top of the scale, a Wilfa electric cooking hotplate of 2 kW (two nominally identical units, labelled A and B, due to the malfunction

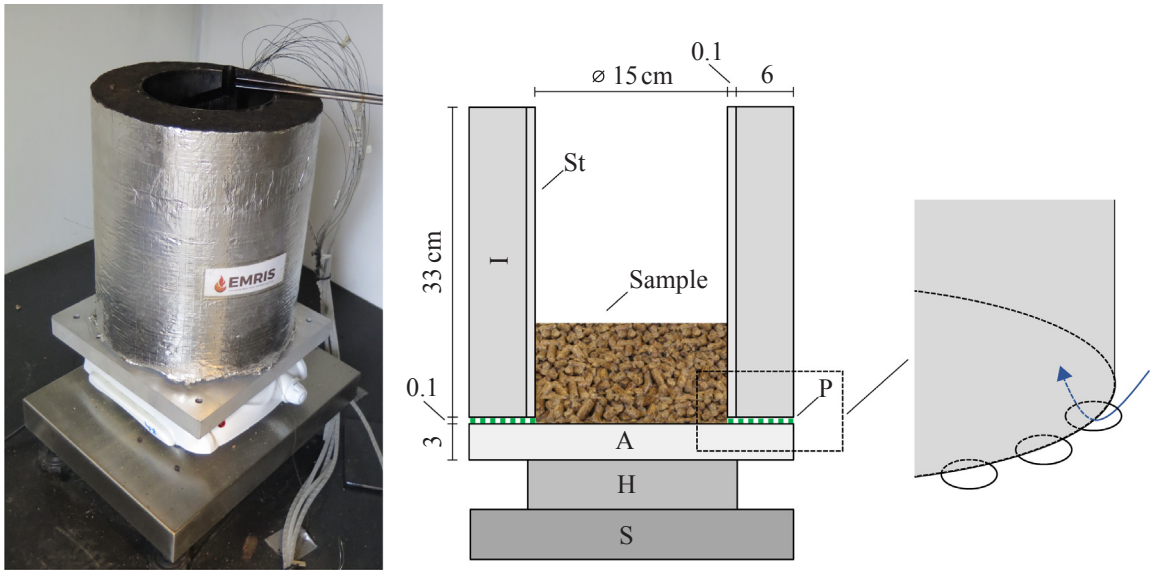

Fig. 1. Experimental set-up. Photo and sketch, from below: scale (S), hotplate/heater (H), aluminium plate (A), perforated steel annulus (P), steel pipe (St) with insulation (I), filled with pellets sample. All dimensions in cm. Smaller sketch: Illustration of the air inlet to the bottom of the cylinder via holes in the perforated annulus.

described in Section 3.1). The heater was controlled by a Jumo B 70.1050.0 digital thermostat (www.jumo.de).

The heater (hotplate) was controlled by the thermostat based on the temperature readings of a thermocouple (Section 2.4) placed under the aluminium plate (next item). In all experiments, the temperature was settled as the maximum reachable by the heater (around 350 °C).

Over the hotplate, a 28 mm aluminium plate (width 28 cm × 28 cm). The aluminium plate had milled channels on its top and bottom surfaces for thermocouples.

On top of the aluminium plate, the steel pipe was placed. The steel pipe was 33 cm high with an inner diameter of 15 cm and wall thickness 1 mm. The insulation around the pipe was 60 mm mineral wool with a density of 140 kg/m^3 and a conductivity of 0.041 W/(m K) and 0.085 W/(m K), respectively, at 50 °C and 300 °C.

A perforated steel annulus, Fig. 2, could be placed between the aluminium plate and the steel pipe. The thickness was 1 mm, inner and outer diameters 14 cm and 24 cm, respectively, with holes of diameter 3 mm and distance 6 mm (centre-to-centre in a triangle). This annulus was used to allow bottom air-draft inlet, and it was removed for the other cases.

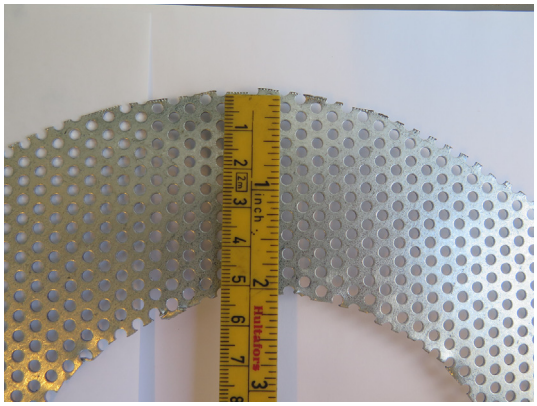

Fig. 2. Section of the perforated steel annulus placed between the aluminium plate and the insulated steel pipe to allow inflow of air to the bottom of the sample. The outer and inner diameters are 24 cm and 14 cm. The holes are 3 mm.

In the centre of the upper opening of the steel pipe, a vertical, bi-directional probe was placed. To prevent melting, the tubing and the pressure transducers were made of metal.

Inside the steel pipe, a ladder with thermocouples was placed (see Section 2.4 below).

A gas measurement unit was placed above the steel pipe.

The two hotplates, A and B, had nominally identical specifications from the producer, while the real characteristics (e.g. actual power developed) may have had some deviations.

2.4. Thermocouples

Type K (chromel-alumel), Class 1, 0.5 mm encapsulated thermocouples (TCs) were used during the experiments. A stainless steel TC ladder was placed inside the pipe, as illustrated in Fig. 3. Temperatures were obtained at 2, 4, 6, 8, 10, 12 and 14 cm height as depicted in the sketch. On each level, the three TCs read the left side (L), centre (C) and right side (R) temperatures with a horizontal separation of 3.75 cm. Another TC was placed at 33 cm, centre position. This arrangement assured that the locations of TCs were fixed during the experiment. In addition, one TC was placed in the centre of the upward surface (0 cm) of the aluminium plate, in a milled channel. Another TC was similarly placed under the plate. In the following, the TC positions are labelled with the height and horizontal position, like “0cmC”, “2cmL”, etc.

Thermocouples are in contact with gas phase and the pellet surfaces, whose temperatures are represented and can be different from the interior pellet temperatures. When gas and pellets surface temperatures differ, the TC will show a temperature between these.

2.5. Gas-flow probe and gas composition measurement

The flow was measured by a bidirectional probe located at the centre line of the pipe [44]. The pressure difference between the two cavities was measured by a pressure transducer with an accuracy of ± 5 Pa and a suitable range of measurement of 0–2000 Pa. The gas temperature near the probe was measured by the thermocouple at 33 cm height.

A device was set up for measuring concentration of O_2, CO_2 and CO at the top opening of the steel pipe, near position 33cmL.

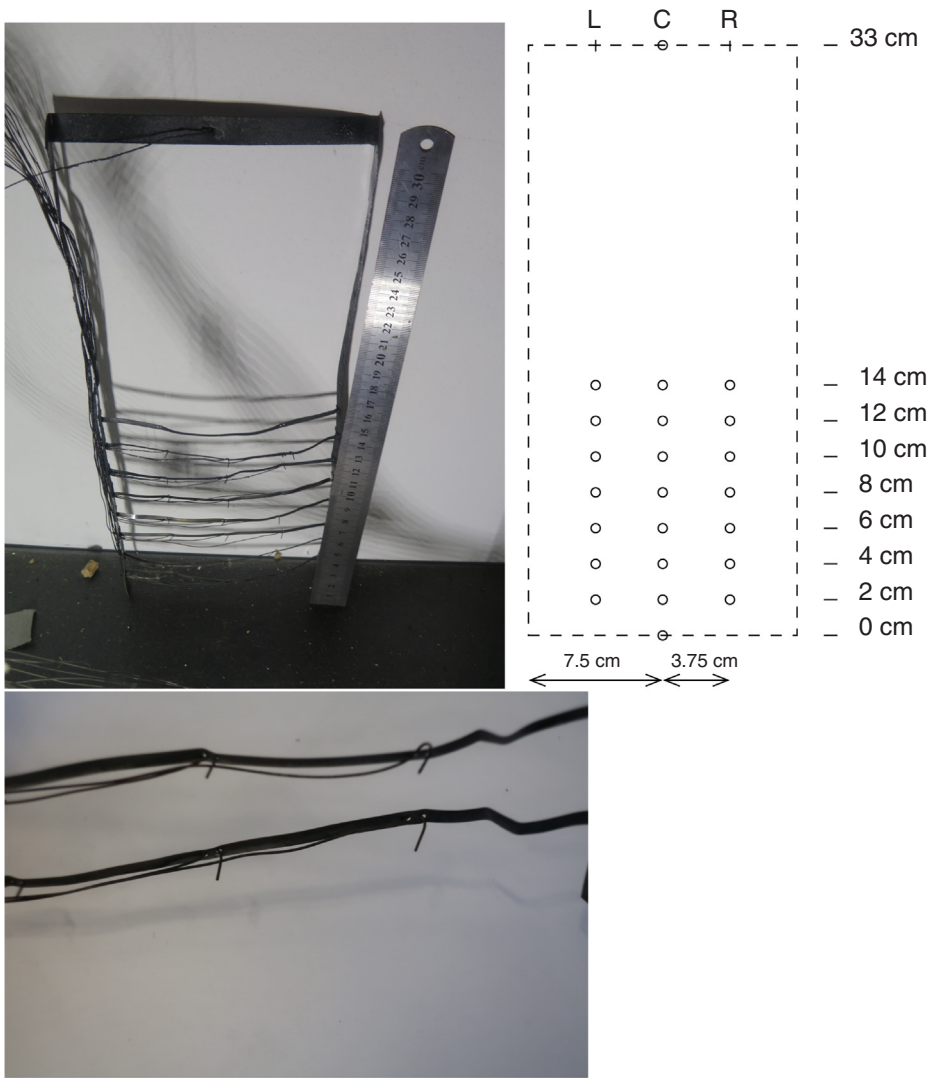

Fig. 3. Thermocouple ladder fixing the thermocouple placement (see text, Section 2.4). In the photo the ruler is 30 cm. The circles in the sketch show the positions of the thermocouples, while the dashed lines indicate the wall, bottom and top of the test pipe. The second photo shows a close-up to some thermocouples attached to the ladder, with the tip positioned mid-air not in direct contact with the ladder.

2.6. Test procedure

The pellets were taken out of the freezer and kept in a sealed plastic bag at room temperature for 3 days in advance to make sure that they thawed without losing their properties. For each test, a sample of 1.25 kg was weighed. This amount corresponded to approximately 10 cm height in the steel pipe. The thermocouple ladder was placed into the steel pipe, and then the pellets were placed inside. The gas measurement unit and the bidirectional probe were placed in the open end of the pipe.

All the tests were run with the same thermostat settings. The logging of mass, temperature, gas composition and air flow was started two minutes before the hotplate was turned on at maximum power. After 6 h, the hotplate was turned off. At the end of the experiment, when all the thermocouples reached room temperature, the logging was stopped. All data were logged every 5 s.

When the test was finished, the remaining sample was removed from the steel pipe and stored. The test equipment (steel pipe and aluminium plate) was washed after each test using a detergent. After a few days, the residue was weighed and sorted manually into two fractions: char and ash. The sorting was made with a 4 mm sieve, which allowed separating ash (the finer fraction) from the black/brown/unburned fuel. After sieving, the fractions were weighted.

3. Results

3.1. Test scheme

The set-up was designed to give upward smouldering propagation in all cases, initiated by heating from below. Placing the perforated annulus between aluminium plate and steel pipe (cf. Section 2.3) allowed air to enter into the bottom of the sample. This gave a buoyant air draft through the sample, in the direction of the smoulder. Hence, a predominantly forward smouldering propagation should be obtained. Without the inlet, the air had to approach the smouldering front from above. Thus, smouldering was in the opposed (aka. reverse) mode. More precisely, the mode was semi-opposed, as there had to be an upward, buoyant gas motion as well.

The labelling of cases in [41] was used. Cases with opposed smouldering, i.e. no bottom air inlet, were identified with labels VR1 to VR12 (R for “reverse”). Ten such cases are reported, as VR4 and VR5 were not completed due to equipment failure. Forward-flow cases, i.e. with bottom air inlet, were identified as VF1 to VF11 (11 cases; F for “forward”). The opposed and forward-flow cases were conducted

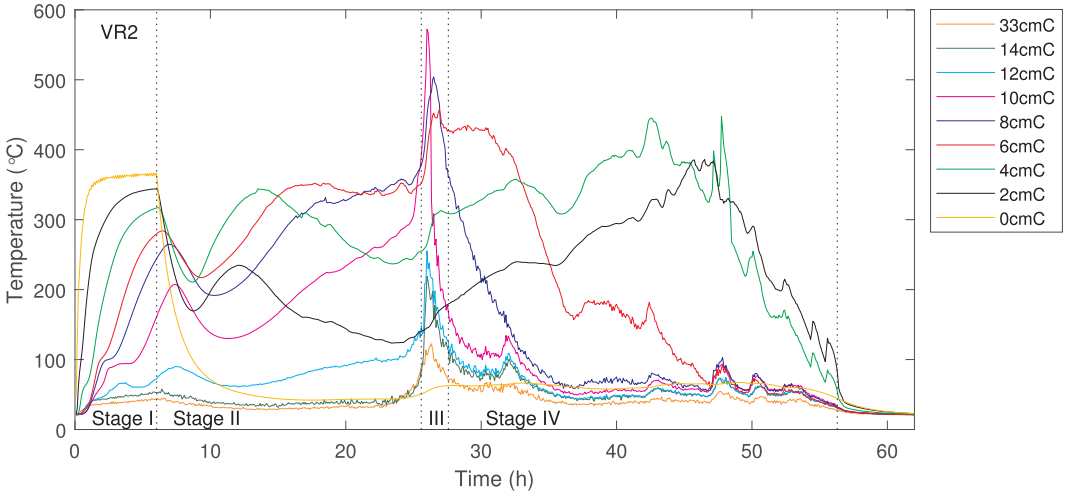

Fig. 4. Temperatures for a case (VR2) of opposed-flow smouldering behaviour. The legend shows the position of each thermocouple. The vertical lines denote the ends of Stages I–IV. (For colours, see the online version.).

alternatingly. The total number of cases was limited by the time available in the project.

It should be noted that the sixth case conducted, Case VF3, gave flaming combustion. Unfortunately, this set fire to the housing of the gas measurement unit, which broke down. Thus, gas composition results were available for Cases VR1-VR3, VF1-VF2. Furthermore, the fire spread to plastics part of the scale, which became less accurate after this incident. In addition, the hotplate was harmed and had to be replaced. Therefore, Cases VR1-VR3 and VF1-VF3 were conducted with Hotplate A, while in the remaining cases, Hotplate B was used.

Some initial tests were also conducted [40] with varying hotplate heating periods. Otherwise, the details were the same. Hotplate A was used. These cases included four without air draft: Two with 4 h external heating, and two with 6 h; and four cases with air draft, with 4 h (two), 6 h and 6.5 h heating. Among these, the two no-draft cases with 4 h heating gave no sustained smouldering, but cooled quietly after the heating. The other six gave smouldering propagation. These results are not reported here, except as trials to settle the main series of experiments and as input to the discussion. The choice of 6 h external heating for the main series was due to the initial tests. Similarly, the failed cases VR4 and VR5 are not reported in detail. However, some of the data may contribute to understanding of smouldering onset.

As mentioned, a pellets bed of some extension will comprise both upward and downward gas motions at different locations within the sample. Thus, the terms opposed and forward will here refer to the net oxygen flow direction, rather than a local or uniform transport of oxygen. In particular, the cases without the bottom air inlet will have a considerable amount both of upward and downward gas flow within the sample. Nevertheless, the net oxygen transport will have to be from the air above the sample, downward to the smouldering front, hence, opposed smoldering. For simplicity, the terms “opposed” and “forward” will be used for, respectively, the cases without and with the air draft from the bottom inlet.

3.2. Observed types of smouldering progress

3.2.1. Stages of the processes

The observed processes could be characterized in four successive stages (I-IV) as follows: The initial 6 h external heating period constituted Stage I. After some time, an intensive combustion period was observed, with a steep increase in temperature. This period was denoted as Stage III. The remaining time intervals were Stage II, before the intensive combustion period, and Stage IV after it. Finally, in a quiet period after Stage IV, the remaining sample cooled to ambient (room) temperature.

As described below, different types of behaviour were observed. All cases without bottom inlet (i.e. opposed flow) followed a scheme where the temperatures were reduced in Stage II after the initial external heating. After several hours, the temperatures rose to Stage III. The draft-inlet (forward flow) cases showed two different behaviours, here denoted as “Type 1” and “Type 2“. Type 1 followed a scheme like that of the opposed-flow cases above. In Type 2, the temperatures (i.e. heat release) started rising within the externally heated period, and Stage III followed directly from Stage I, with no Stage II.

The beginning of Stage III was set to the first instance where any temperature of the sample exceeded 450 °C and the duration of this period was set to 2 h. This time span captured most of the intensive combustion in all cases. For the analysis of data, the duration of Stage I was truncated by Stage III, when this occurred before the end of 6 h external heating.

The end of Stage IV was set to the instance when all temperatures had fallen below 125 °C, without any later increase. The latter limit was somewhat arbitrary. However, the choice served to distinguish between active and non-active periods of the process.

The volume was not metered. Nevertheless, visual observations indicated that it remained approximately constant during Stages I and II, possibly with some swelling and shrinking. Hence, the mass loss mainly led to reduced bulk density. During Stage III, the volume reduction was considerable, with partial collapse, both of individual pellets and of the bulk stacking of pellets. This period was characterized by strong emissions of smoke. During Stage IV, the reduction was modest. These observations were made by human eye, assisted by the fixed thermocouple ladder, Section 2.4. Furthermore, the temperature readings of thermocouples in the gas volume above the sample were seen to fluctuate more rapidly than those known to be within the sample. This behaviour indicated when the sample had sunken below a certain thermocouple position.

The opposed-flow cases lasted for 54–65 h before reaching ambient temperature, while those with air inlet lasted for 31–38 h (Type 1) or 17–22 h (Type 2).

3.2.2. Smouldering behaviour without air-draft inlet: opposed ropagation

Fig. 4 shows the transient temperatures of an example (Case VR2) of opposed behaviour, while Fig. 5 shows the mass depletion. Here, and in following graphs, the vertical dotted lines in the graph denote the end of Stages I to IV. The legend entries denote thermocouple positions in cm above the bottom plate (cf. Section 2.4 and Fig. 3). The 12, 14 and 33 cm thermocouples were located above the sample.

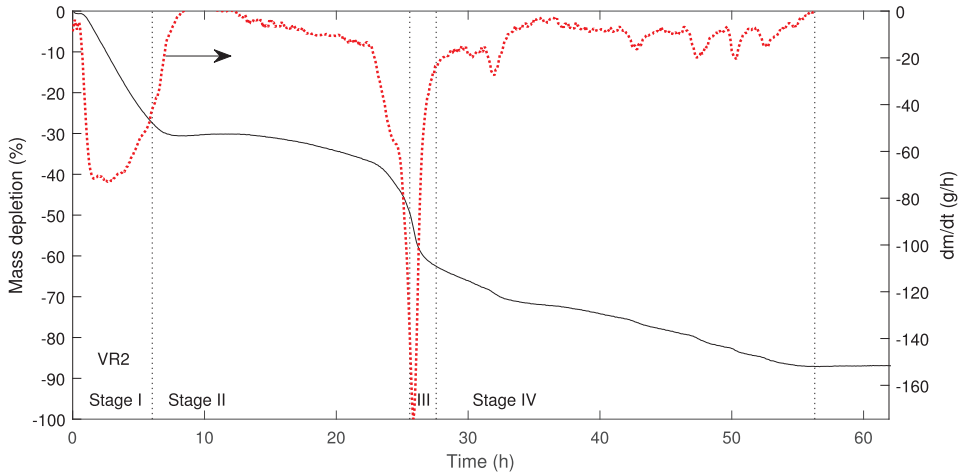

Fig. 5. Sample mass loss (left axis) and mass loss rate (right axis) of Case VR2, opposed-flow smouldering. The vertical lines denote the ends of Stages I–IV.

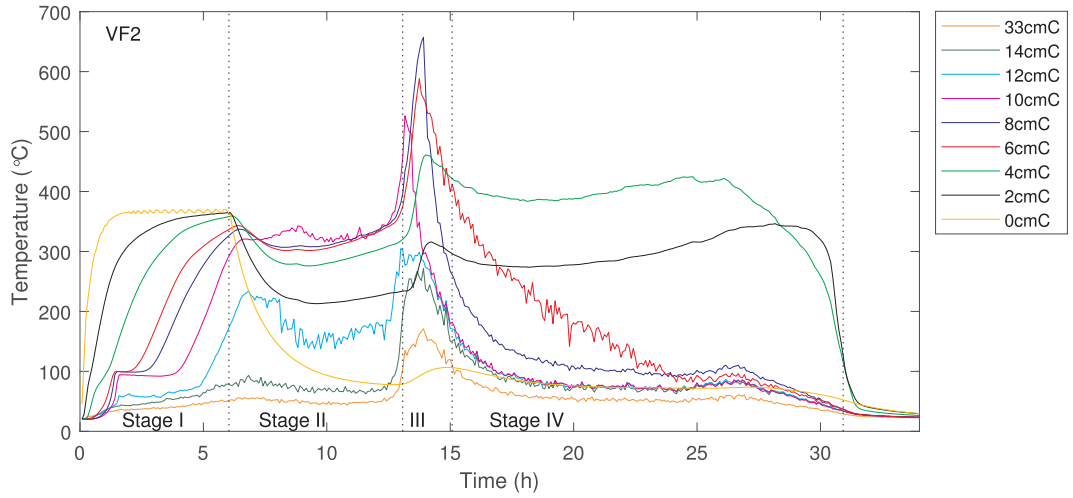

Fig. 6. Temperatures for a case (VF2) of forward smouldering behaviour Type 1 (see caption of Fig. 4).

During the externally heated period, here identical to Stage I, the temperature of the aluminium plate (position 0 cm) reached its maximum value. This was followed successively by TCs at 2–12 cm height, which reached intermediate peak temperatures at or just after the end of Stage I. The three horizontal TC positions (L, C and R) showed slightly different heating paths, as the pellet distribution within the pipe was not fully uniform. Generally, the centre TC had the highest temperature among the three horizontal positions.

The sample cooled during the first hours of Stage II, followed by a turnaround period that maintained an approximately constant temperature in this period, before a rapid increase towards the high temperatures in Stage III. In the cases of opposed flow, Stage II lasted for 19–23 h (exception: 26 h for one case). The TCs alternated around 250 °C with the exception of the 2 cm position, which cooled together with the bottom aluminium plate and hotplate (not insulated). The maximum temperature in this period was registered in the TCs located in the pipe centre at 8 and 10 cm height. In the case shown (Case VR2, Fig. 4), the 2 and 4 cm heights reached intermediate peak temperatures at 360 °C before declining again. In this case, the mass was virtually constant for several hours of Stage II, before a slow decrease. At the end of Stage II, the mass loss rate increased notably some time prior to the onset of the corresponding temperature rise towards Stage III.

In Stage III of this case, the maximum temperature reached 591 °C after 28.3 h. All TCs at 8 to 33 cm height had their maxima in this period. The temperature increase towards Stage III set on simultaneously in the upper half of the sample (6–10 cm). This occurred after a long period (10–15 h), where the 6 and 8 cm positions had relatively stable temperatures of 300–350 °C. In most opposed-flow cases, the 6 and 8 cm levels reached 400 °C at the time when the 10 cm level went into a rapid increase from about 250 °C towards its peak temperature. In the same period, the mass depletion rate gradually increased (Fig. 5). The combination of changed composition (towards char) and increased porosity within the individual pellets, giving more access to oxygen, might have led to the enhanced reaction rates. During Stage III, the lower part of the sample barely exceeded 200 °C and 300 °C, respectively, at 2 and 4 cm.

During Stage IV, the TC readings at 2–6 cm showed some irregular rise and fall as the reaction was proceeding. The behaviour could be explained by local collapses of the bed, with supply of air from above. These positions had their maximum temperatures in this period. Typically, the 6 cm TCs showed higher values early in Stage IV, while TCs at 2 and 4 cm showed peak values later in the period. The readings at 8–10 cm, subsequently also 6 cm, indicated that these positions were above the sample. This was visually observed, as well.

3.2.3. *Forward smouldering behaviour Type 1*

Two out of eleven experiments with air draft from below developed a Type 1 behaviour. Fig. 6 shows one of these, Case VF2. As seen, the TC readings in the upper part of the sample showed a more distinct plateau at 100 °C compared to the opposed flow. Furthermore, due to the upward airflow, the temperatures inside the sample became higher during the external heating period. The corresponding mass depletion is shown

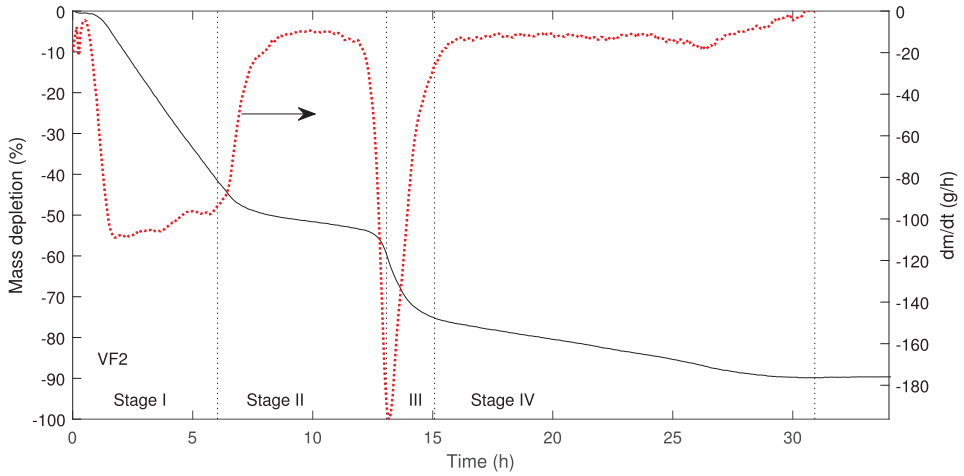

Fig. 7. Sample mass loss (left axis) and mass loss rate (right axis) of Case VF2, forward-flow smouldering Type 1. The vertical lines denote the ends of Stages I–IV.

in Fig. 7. Additionally, three of four initial cases (Section 3.1) gave this behaviour, two of 4 h external heating and one of 6 h.

During Stage II, the sample cooled by approximately 60 °C and then underwent a period of relatively steady temperature for 5 h. The temperatures were approximately 300 °C in this particular case. In Stage III the temperature increased to a maximum of 670 °C after 13.8 h. This stage was initiated by an increase in the upper layers of the sample (6–10 cm), which had a rapid temperature increase from about 350 °C in Stage II towards their peak temperatures in Stage III. The positions 4 and 2 cm followed with delay and to lower peak temperatures, although higher than those seen for the opposed-flow cases (Section 3.2.2).

The final Stage IV was similar to the no-draft cases, although shorter and less irregular.

3.2.4. Forward smouldering behaviour Type 2

Eight out of eleven test runs gave this behaviour, and Fig. 8 shows the temperatures of an example (Case VF5). Unlike the previous two behaviours, the sample rose to higher temperatures during the external heating. Already at 1.9 h in this case, sample temperatures exceeded that of the aluminium plate (0 cm).

The temperatures started to increase most rapidly at the bottom of the sample (2 cm), and the upper layers of the sample followed. This type had no Stage II, as Stage III commenced before the end of the external heating. For all cases, the temperatures of 400–450 °C, in some cases also 500 °C, were first reached at the positions 2–4 cm. Subsequently, those at 8–10 cm had a rapid increase, and reached 600 and 700 °C. The following Stage IV was similar to the cases described above, altough with a shorter elapse time.

The mass depletion graphs of the Type 2 cases were similar to those above, except that the decrease in Stage III continued directly from that of Stage I.

3.2.5. Flaming fire

One test run, Case VF3, developed for sure into flaming fire. The incident was observed as the TCs above the sample (12 and 14 cm) gave temperatures above 800 °C for a period of 4 min at time 5.17 h. Furthermore, the TC at 33 cm, located well above the sample, showed a high temperature of 776 °C. In all other cases, the 33 cm temperature was much lower (150–300 °C). At closer inspection, it was seen that a hot spot developed at 2 cm, which came above 800 °C at time 5.03 h and rose rapidly to a peak of 943 °C. The elevated temperature propagated upward through the sample in a few minutes. In addition, the bottom aluminium plate was considerably heated by the combustion.

Except for the higher temperatures and shorter total duration time, the behaviour of this case was similar to Type 2 above.

3.2.6. Non-sustained smouldering cases

Two cases investigated did not give sustained smouldering, which indicated on the limits of heating and/or time of heating required to reach sustained smouldering. Due to the equipment degradation, these cases had lower temperatures after the external heating. The aluminium plate (0 cm) reached 290 °C in both cases, and the sample (2 cm)

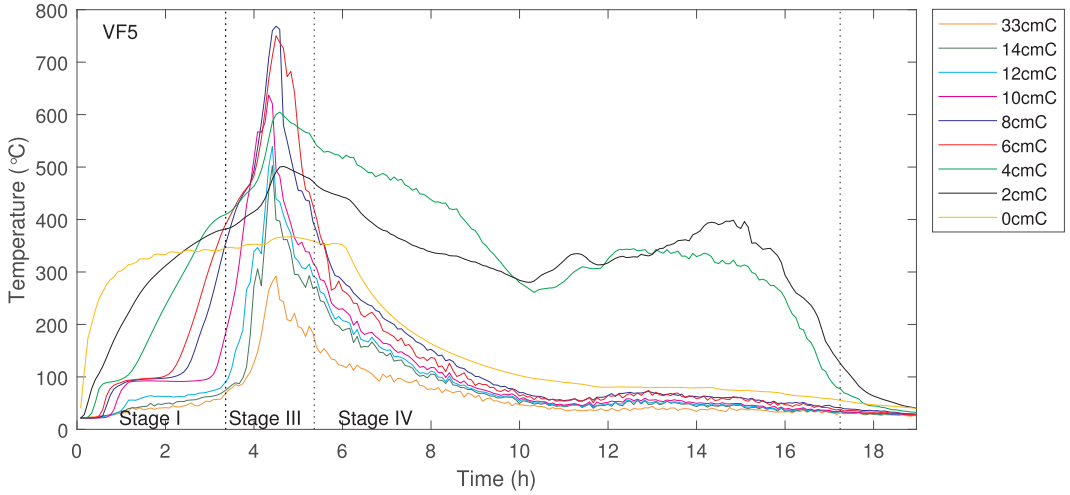

Fig. 8. Temperatures for a case (VF5) of forward smouldering behaviour Type 2 (see caption of Fig. 4).

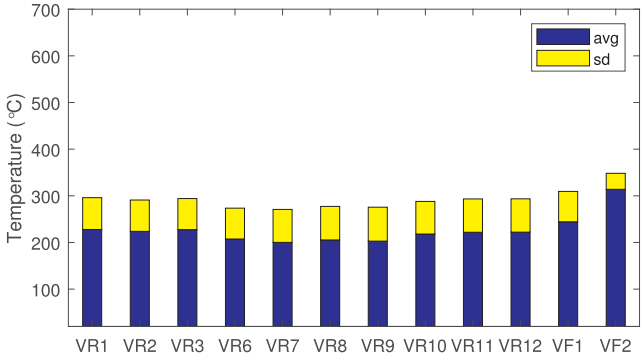

Fig. 9. Mean and standard deviation of all temperatures recorded at 2–10 cm height in Stage II for opposed flow (VR1-VR12) and forward flow Type 1 (VF1-VF2).

reached 275 °C after 6 h. The monotonic cooling reached 125 °C at about 9 h and continued to room temperature.

Two of the initial cases had external heating for 4 h, where the aluminium plate (0 cm thermocouple) reached 360 °C, and the sample (2 cm) reached 230 °C. Both cooled monotonically after the heating, reached 125 °C at 8.2–8.3 h and finally the room temperature. These cases had a mass loss of 18–19% at 4 h and lost another 4% in the following 1–1.5 h.

3.3. Temperatures

3.3.1. Temperature levels and variation

Mean (arithmetic) and standard deviations of temperatures within Stages II (2–10 cm heights), III (2–10 cm) and IV (2–4 cm) were calculated for all cases and shown in Figs. 9–11, respectively. These illustrate the temperature levels in the stages and the repeatability of the cases. Although some variation, there were close similarities among cases of the same type, and distinct differences between cases of different types.

The maximum temperatures for each period are shown in Table 1 for the cases of opposed flow and in Table 2 for the cases of forward flow. In addition, the location of the thermocouple measuring this value and the instance of time are included in the tables. For the period preceding the intensive Stage III (i.e. Stage II if observed, else Stage I), the maximum temperatures were just below 450 °C and occurred just before the initiation of Stage III, according to the applied criterion for this stage.

The temperature-time and mass-time diagrams above were made by extracting every 60th data point. Due to this, in the temperature diagram, some high peaks were not captured by the graphs. This explains the differences in maximum temperatures between the temperature-time graphs and tables and graphs based on all data. Shorter data extraction intervals gave similar graphs, but visually with thicker lines.

3.3.2. Horizontal variation of temperature measurements

In order to evaluate the horizontal deviation, the average and root-mean-square (RMS) values were calculated of the temperature deviations, $(T_L - T_C)$ and $(T_R - T_C)$ for each height (thermocouple positions from 2 cm to 12 cm) within each of the Stages I-IV. Here, the subscripts L, C and R refer to the thermocouple positions, see Section 2.4.

In Stage I, deviations were small (mostly 8–12 K as RMS), with some exceptions for Type 2 forward cases since smouldering propagation set on before the end of external heating.

In Stage II, the opposed-flow cases showed consistently lower temperatures T_L and T_R compared to T_C (mostly in range 40–100 K, RMS). This was also observed for Type 1 forward in the upper part of the sample, while the lower part showed results that were more mixed.

In Stage III, opposed-flow, the deviations were more negative than positive. T_L was consistently lower than T_C, while T_R was more up and down in relation. For forward Type 2, the lower positions (2–4 cm) had consistently positive deviations for L and R, while the upper part and Type 1 results were mixed.

Fig. 12 shows the temperatures T_R, T_C and T_L at 4 and 8 cm height for Stages I-III of two cases. It was seen that in Stage II, the opposed flow (no draft inlet) case had generally larger horizontal differences than the forward flow case, while lesser in Stage I. Examples of horizontal temperature profiles are shown in Fig. 13 for two instances (5.0 h and 12.0 h) for the same cases. In particular, the 12.0 h examples showed notable horizontal temperature differences.

3.3.3. Temperature gradients in the externally heated period

A particular observation was made on the temporal temperature gradients (aka. heating rates) in the externally heated period, where temperatures rose from 100 °C to 200–300 °C. For the opposed-flow cases (VR1-VR12) the gradient at 2 cm height was 2.5–3.0 K/min and at 8 cm, 0.5–0.9 K/min. These locations reached temperatures at 300–320 °C (2 cm) and 200–250 °C (8 cm) in Stage I, before cooling again. Apparently, this was sufficient to cause resumed and sustained smouldering 2–4 h later. The non-sustained Case VR4 had lower values: 1.6 K/min to 270 °C at 2 cm, and 0.4 K/min to 160 °C at 8 cm. For the forward cases (VF1-VF11), at 2 cm, the gradient was similarly in the range 2.5–3.3 K/min to approximately 300 °C before either intermediate cooling or further increase due to reaction heat. At 8 cm, a difference was seen between Cases VF1-VF2 (0.9–1.4 K/min, reaching 200–250 °C before intermediate cooling) and Cases VF3-VF11 (2.8–4.0 K/min to approx. 300 °C, and then continuing directly into the intensive Stage III).

3.4. Reactions, heat and mass transfer

In this section, simple estimates based on known relations from combustion, heat and mass transfer and order-of-magnitude calculations are used to clarify whether certain features are plausible, or whether specific factors are of importance or not.

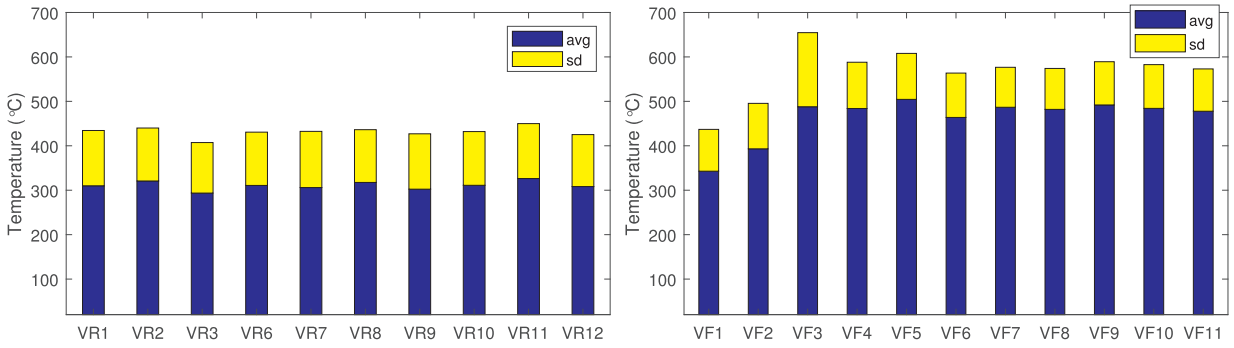

Fig. 10. Mean and standard deviation of all temperatures recorded at 2–10 cm height in Stage III. Opposed (VR) and forward flow (VF).

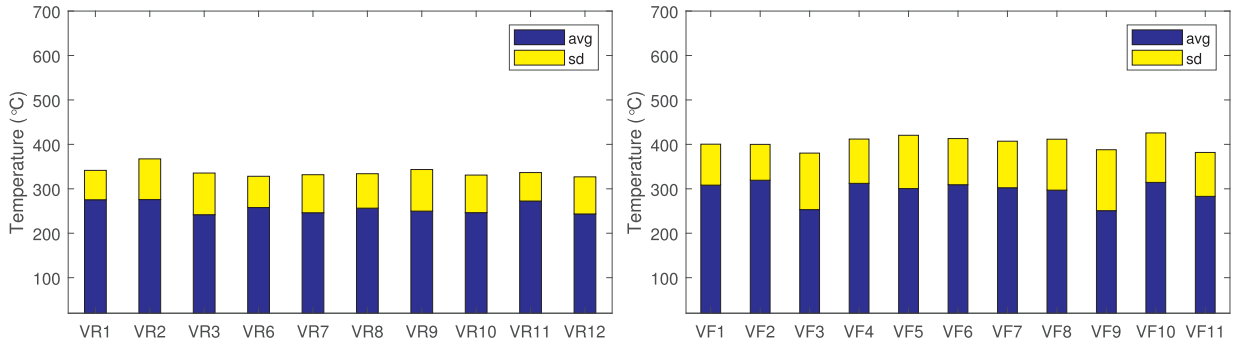

Fig. 11. Average and standard deviation of all temperatures at 2–4 cm height recorded in Stage IV. Opposed (VR) and forward flow (VF).

3.4.1. Energy transfer and conversion

The hotplate (2 kW) appeared to give full power for a good hour and then for roughly half of the remaining time until it was turned off at 6 h. That is, a release of 25 MJ. For a comparison, an approximation was made for the heat absorbed and stored by equipment and sample. After the external heating period, the temperatures of the aluminium plate and the samples of the opposed-flow cases were on average increased by approximately 340 K and 185 K, respectively. Furthermore, the sample mass was reduced by approximately 30%, that is, 0.09 kg water and 0.30 kg volatiles out of a 1.25 kg sample.

When assuming that the steel pipe was heated like the sample, and assuming typical specific heats and enthalpies of evaporation, it was estimated that the temperature increase corresponded to 2.5 MJ and the evaporation to 0.9 MJ. That is, less than 15% of the heat from the hotplate, and even less when oxidation of volatiles are considered. Accordingly, a considerable amount of heat was dispersed into the surroundings.

The heat losses through the insulated sidewall of the test pipe were estimated to an order of magnitude of 0.01 MJ/h or less for the temperatures relevant for the entire experiment. This estimate was based on the geometry, conductivity of the insulation, a Nusselt number correlation [45,46] and properties of air. Accordingly, these heat losses were insignificant.

After external heating, the aluminium plate temperature fell markedly and relatively fast (see e.g. Fig. 12, temperature at 0 cm), which demonstrated that the heat losses from it and the hotplate were considerable. Another potential heat loss mechanism was the gas flow into and out of the sample. This will be discussed below.

For a comparison, the volume of the test pipe (6 l) corresponds to the combustor of a commercial 50 kW burner [47,48], which will consume the sample of 1.25 kg pellets completely in 7 min.

3.4.2. Gas flow velocities and gas composition

Since the sample filled about 10 cm of the 33 cm steel test pipe (cf. Fig. 1), the upper part formed a cavity filled by air and flue gases. The typical value for the measured air flows at 33 cm after the external-heating period were either upwards near 0.3 m/s (Cases VR6-VR12 and VF4-VF12) or the same value downwards (Cases VR1-VR3, VF1-VF3). The instantaneous values were found to fluctuate around the typical value.

The gas component measurements were fluctuating, which obviously resulted from the varying gas motions mentioned. Hence, they were regarded as unsatisfactory to represent quantitatively the effluents from smouldering and are not reported in detail. Nevertheless, the tendencies were that O_2 was intermediately reduced in Stages I and III, but still with a relatively large value (above 15%). CO_2 and CO increased during Stages I and III, while having a lower, but still notable, value in Stages II and IV. Furthermore, the level of CO was found to be low, 2 to 3 orders of magnitude less than CO_2. This ratio fluctuated, but did not show particular tendencies except an increase during the first 1–2 h of Stage I.

No particular wind sounds were observed during the experiments. This indicated a low velocity in the passage through the perforated annulus between the aluminium plate and the steel pipe for forward flow (Section 2.3 and Fig. 1). An estimate of the air-draft flow into the sample can be made by integrating the Euler equation through the passage, into the sample and to the outlet of the pipe. Without the flow resistance in the sample, the estimate was 1.5 m/s. That is, with the resistance included, realistically well below 1 m/s. An air mass inflow of $0.1{\cdot}10^{-3}$ kg/s turned out as a higher limit. This was much less than required for the smouldering process, especially in the period of intensive reactions, Stage III.

3.4.3. Gas-phase reactions

In comparison with the timescale of the smouldering process (hours), the timescales of gas-phase chemical reactions can be assumed very fast. Above, the turbulent motions were estimated to a timescale of 1 s. Time scales of the global reaction of CO with O_2 were estimated

Table 1
Maximum temperature, its position and time for Stages I-IV, opposed-flow cases.

Stage	I			II			III			IV		
Case	T_{max} (°C)	Pos.	Time (h)	T_{max} (°C)	Pos.	Time (h)	T_{max} (°C)	Pos.	Time (h)	T_{max} (°C)	Pos.	Time (h)
VR1	344	2cmC	6.00	449	10cmC	27.79	591	10cmR	28.30	546	6cmR	43.18
VR2	344	2cmC	6.02	450	10cmR	25.57	595	10cmC	26.13	505	8cmL	30.91
VR3	347	2cmC	6.00	447	10cmR	25.23	522	10cmR	25.52	574	8cmC	27.96
VR6	327	2cmC	6.01	449	8cmC	28.27	558	10cmL	28.63	460	6cmC	32.19
VR7	310	2cmC	6.01	449	8cmR	28.13	604	10cmL	28.82	505	8cmL	30.13
VR8	312	2cmC	6.03	449	10cmL	32.09	587	10cmL	32.30	611	6cmL	47.89
VR9	307	2cmC	6.01	447	10cmR	29.31	593	10cmL	29.57	506	6cmL	53.73
VR10	306	2cmC	6.00	450	8cmC	25.04	632	10cmL	25.73	514	4cmR	50.53
VR11	306	2cmC	6.03	449	8cmC	27.56	635	10cmL	27.87	487	6cmC	30.16
VR12	306	2cmC	6.03	447	8cmC	29.25	554	8cmC	29.77	499	6cmC	31.37

Table 2
Maximum temperature, its position and time for Stages I–IV, forward-flow cases.

Stage	I			II			III			IV		
Case	T_{max} (°C)	Pos.	Time (h)	T_{max} (°C)	Pos.	Time (h)	T_{max} (°C)	Pos.	Time (h)	T_{max} (°C)	Pos.	Time (h)
VF1	338	2cmR	6.03	447	8cmR	21.37	604	8cmL	22.56	483	6cmL	23.44
VF2	381	2cmL	6.03	449	10cmR	12.88	670	10cmC	13.79	440	4cmR	15.22
VF3	450	2cmR	4.78	–	–	–	943	2cmR	5.10	535	4cmR	6.79
VF4	450	4cmL	4.31	–	–	–	760	8cmR	5.35	508	4cmC	6.31
VF5	450	4cmR	3.36	–	–	–	801	8cmC	4.46	582	4cmR	5.40
VF6	446	10cmR	4.73	–	–	–	723	8cmC	5.48	485	4cmR	6.75
VF7	450	4cmL	4.82	–	–	–	776	8cmC	5.81	529	4cmR	6.91
VF8	450	4cmR	4.27	–	–	–	790	8cmC	5.14	519	4cmR	6.28
VF9	450	4cmL	3.46	–	–	–	765	8cmC	4.40	618	4cmR	5.56
VF10	450	4cmL	4.32	–	–	–	796	6cmR	5.40	519	4cmR	6.32
VF11	449	4cmR	4.36	–	–	–	735	8cmC	5.49	567	4cmR	6.64

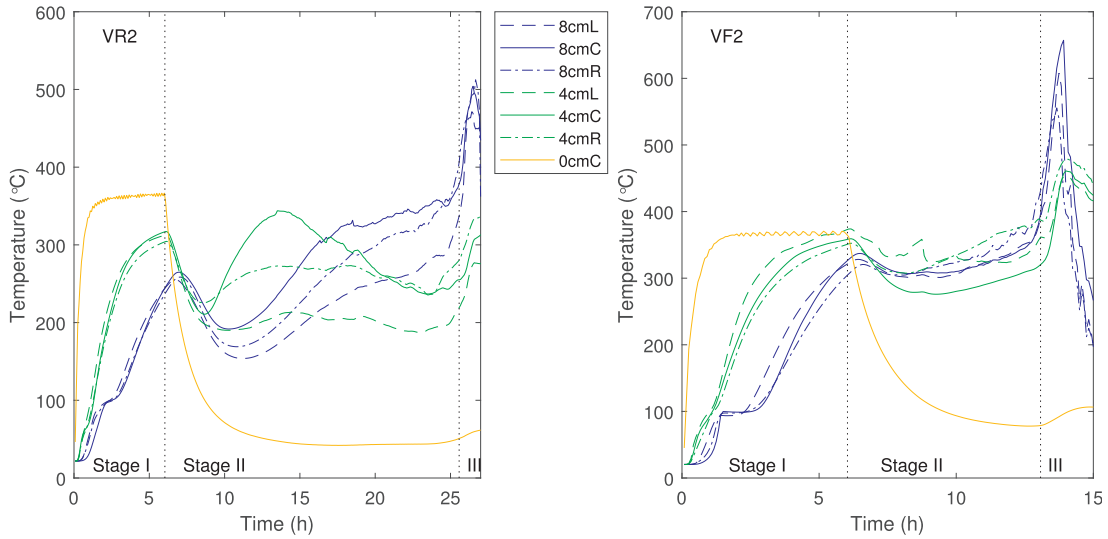

Fig. 12. Temperatures at different horizontal locations at 4 and 8 cm height, for an opposed flow case (VR2, cf. Fig. 4 and a Type 1 forward flow case (VF2, cf. Fig. 6).

(e.g., Turns [49] p. 129 et seq.) on the basis of the mechanism of Westbrook and Dryer [50]. At a temperature of 350 °C, the estimated timescale was 0.5 s, or (with excess of O_2) less. For higher temperatures, the timescale was much smaller (e.g. 0.05 s at 400 °C) due to exponential relations. Within realistic concentrations, the estimate was not notably sensitive to composition of the gas. This means that whenever O_2 is available, the pyrolysis products will be consumed fast (relative to the smouldering timescale) towards equilibrium. Furthermore, at the relevant temperatures (< 1000 K), the CO-CO_2 equilibrium is strongly in favour of CO_2 (10 orders of magnitude or more).

3.5. Propagation of fronts

The spreading of drying, pyrolysis and oxidation in organic fuels can be indicated [51] by observing the fronts of 100 °C, 200 °C and 350 °C, respectively. The time to reach 100 °C and 200 °C at different heights in the centre of the sample is shown in Fig. 14. The graph shows averages within all opposed-flow cases and all Type 2 forward-flow cases (VF4-VF11). Variations among cases are indicated by the error bars, which show standard deviations. For 100 °C, Type 1 forward was similar to the opposed flow and is not shown.

It should be kept in mind that the external heating from below lasted for 6 h. Furthermore, it is noted that the low number of cases makes the standard deviations to indications of variation rather than statistical quantities. The front spreading speeds calculated from the average times of propagation in Fig. 14 are shown in Fig. 15.

The times to reach temperature 350 °C, which represents oxidation [51], are shown in Fig. 16. For forward flow Type 2, this temperature occurred within the externally heated period (6 h). Moreover, in the opposed flow cases, some locations (2–4 cm, sometimes 6 and 10 cm) did not reach 350 °C within Stage II, as seen from Fig. 4. For these instances, the time to the intermediate maximum was used in the graphs of Fig. 16. The Type 2 forward flow cases showed 350 °C propagation speeds of 3–25 cm/h. In the majority of instances, the opposed flow had propagation speeds that were an order of magnitude lower, within 0.13–3.1 cm/h. The latter was relatively low compared to some other studies (on powder) [12,17], while more in the range of [16,25]. For some instances, however, the 350 °C temperature was reached nearly simultaneously at two heights.

3.6. Residues

The opposed-flow cases gave on average 17 g ash (fine fraction) and 155 g char (coarser), or 1.4% and 12.4%, respectively, of the original sample mass. The Type 1 forward cases left 2.0% ash and 9.0% char, while for the Type 2 forward cases, the residues were 1.7% and 7.4% on average. The flaming case (VF3) gave 1.4% ash and 6.3% char.

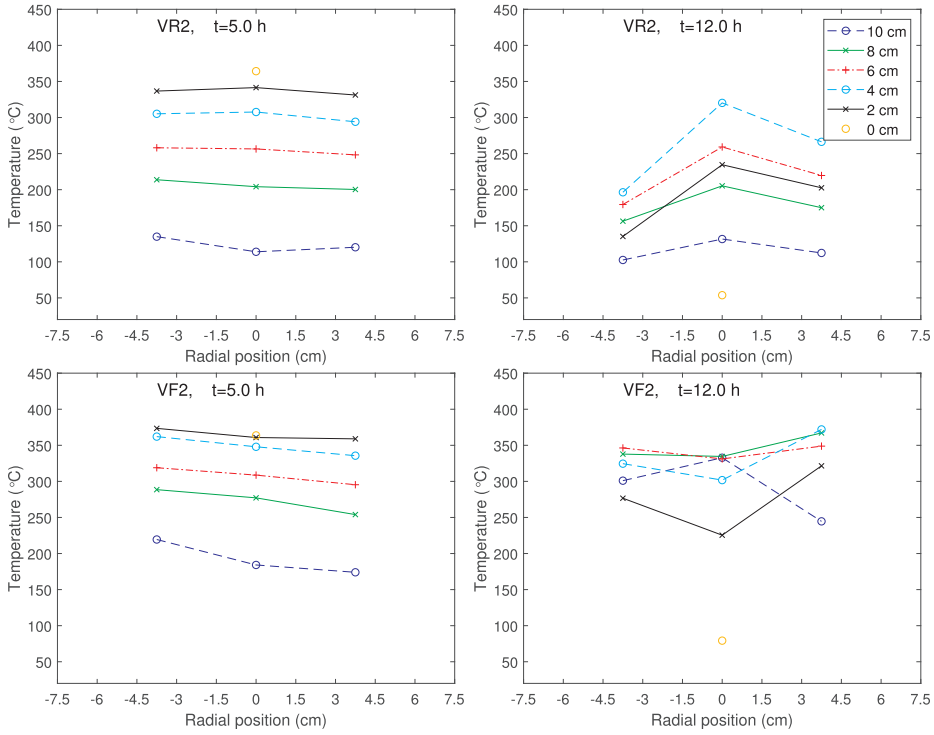

Fig. 13. Horizontal temperature profiles at different heights for the opposed flow Case VR2 and forward flow Case VF2 (cf. Fig. 12) at 5 and 12 h. The horizontal extent of the graphs corresponds to the inside diameter of the test pipe.

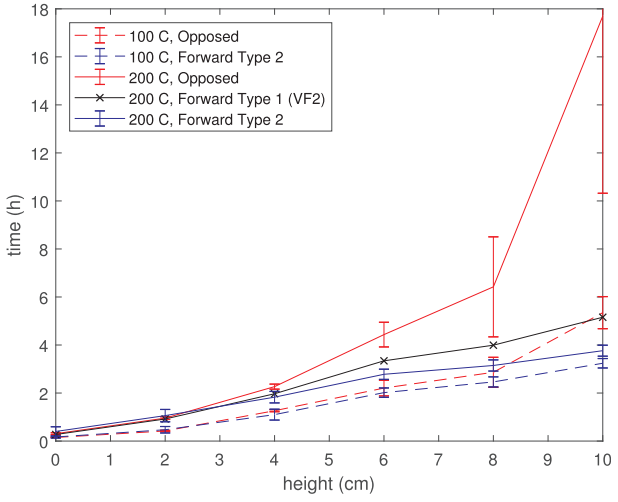

Fig. 14. Time to reach 100 °C and 200 °C at different heights in the centre of the sample. Average values for each type. Error bars show standard deviations.

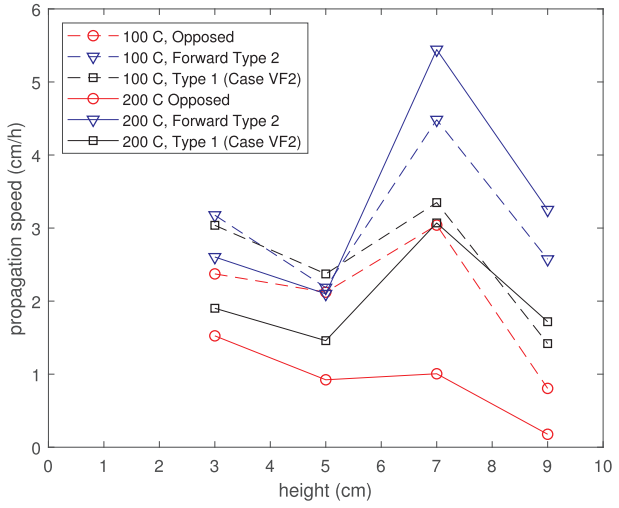

Fig. 15. Propagation speeds of 100 °C and 200 °C fronts at different heights in the centre of the sample based on average values.

4. Discussion

4.1. Frequency of data

Recording data every 5 s meant that very short-lasting events were not captured, such as short outbursts of burning gas. On the other hand, the main processes of smouldering take place on much longer timescales, on the order of hours rather than seconds. An exception was the flow in the gas phase above the sample. The readings of thermocouples located here must be regarded as average temperature values rather than fluctuations. Even here, the timescales of turbulent motions (estimated [52] to an order of magnitude of 1 s, based on size and measured velocity) were quite large compared to those that can be found in turbulent flames.

4.2. Gas flows within and above the pellets bed

The horizontal temperature differences shown (Section 3.3.2, Figs. 12 and 13) could set up upwelling flows through the porous material. At least for the configuration without inflow from bottom, these upward flows led to downdraft in other parts of the sample. Hence, fresh air can be brought into the sample to initiate and enhance smouldering. For the forward-flow configuration, the temperature differences will enhance and modify the buoyant flow through the sample. Also for these cases, downdraft flow was a possibility. During the external heating period, the steel test tube temperature presumably approached that of the aluminum plate (Thermocouple 0cmC). This must have enhanced upstream flows near the wall and thereby contributed to the internal flows.

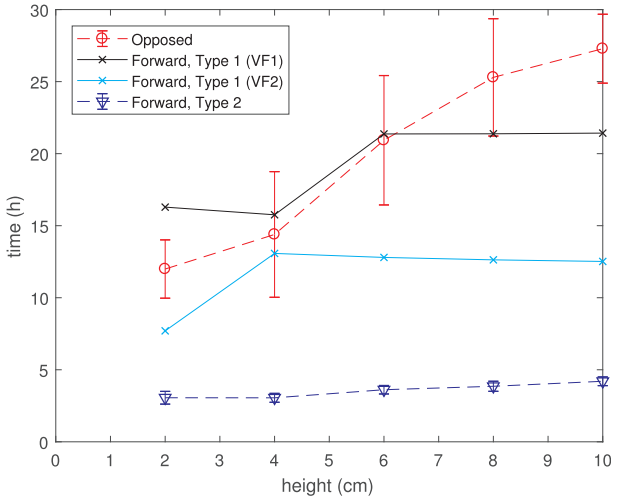

Fig. 16. Average time to reach 350 °C (or the lower intermediate peak temperature in Stage II if relevant) at different heights in the centre of the sample. Error bars show standard deviations.

In Section 3.5, it was seen that for some instances, the temperature assumed for oxidation (350 °C) was reached nearly simultaneously at two heights. This indicated that the smouldering could spread as a distributed reaction rather than a distinct front. In addition, the Type 2 forward cases with the higher propagation speed (approx. 25 cm/h) can be interpreted in this manner.

Although limited, the available data (Section 3.4.2) on gas flows were consistent with irregular, fluctuating and circulating motions above the sample. The data showed that air flows from above gave a supply of fresh air into the cavity. Furthermore, the low CO-to-CO_2 ratios and the relatively high O_2 contents observed indicated that the reactions occurred at excess oxygen and to a high degree of completeness.

The estimates on gas-phase reactions (Section 3.4.3) show that very low CO concentrations should be expected above the sample. Generally, CH_4 and H_2 are more reactive and will be consumed before CO. Furthermore, as long as oxygen is available, notable gas-phase reactions will take place within the void of the pellets sample. Here, it should be kept in mind that 42% of the dry fuel is oxygen (cf. Section 2.1).

4.3. Type 1 vs. Type 2 forward smouldering

An idea for explaining the development of Type 1 vs. Type 2 behaviour was that the initial temperature development might have been different. Furthermore, it is plausible to ask if the change of hotplate after VF3 can be a reason. However, inspecting the temperature development of the aluminium plate and the sample in Stage I, showed that VF1 had a lower externally heated temperature than VF4-VF11, whereas VF2 had a higher temperature. It can also be pointed out that among the initial cases (all conducted with Hotplate A), both Type 1 and Type 2 behaviour were observed.

Another possible aspect can be the quality of the pellets samples, such as wood-species mixture, wood growing condition, trunk vs. branches, etc. The specifications of the delivered fuel were not sufficiently detailed to judge this. Furthermore, differences in the irregular stacking of the pellets sample is a possibility.

The development of smouldering combustion is a composite process including heat and mass transfer (Section 2.2), pyrolysis, chemical reactions, gas motion within and above the sample, etc. On one hand, the gas flow within the sample can supply oxygen to the reaction. On the other hand, the same gas flow can cool the individual pellets inside the sample. The relatively low propagation speeds indicated that the latter effect was important.

It is worth noting (Section 3.3.3) the differences at 8 cm between Type 1 (Cases VF1-VF2) and Type 2 (Cases VF4-VF11) forward smouldering. The faster heating of the upper part of the sample may be part of the explanation of the different behaviours. Data by Anca-Couce et al. [53] showed that when the heating rate was reduced from 10 to 2.5 K/min, the depletion and depletion rate of wood in air was reduced. However, the effect was seen mainly at higher temperatures, while for 250–300 °C, the gasification at 2.5 K/min was moderately less than that at 5 and 10 K/min. Experiments by Kashiwagi and Nambu [54] showed similar results for paper in air for heating rates of 1, 3 and 5 K/min.

Faster heating and more intense pyrolysis and oxidation are self-reinforcing processes. The initial cause of the larger temperature gradient can possibly be the properties of the sample, such as composition, size (i.e. length) of pellets and stacking of the sample. Different air flow patterns due to different stacking of pellets affect oxidation, heat transfer and species mass transfer.

Initation of combustion (smouldering or flaming) depends on the reaction rate of the solid and the evaporated volatiles (usually exponential in temperature), heating/cooling of the reactants, and supply and removal of gaseous reactants. A gas flow will both supply air, heat or cool the fuel, and remove (or supply from upstream) evaporated volatiles and combustible reaction products.

A study of van Blijderveen et al. [55] on ignition of wood chips in packed beds heated by an air flow showed spontaneous ignition in the range 225–250 °C. A lower air velocity (i.e. lower rate of heat transfer) gave lower ignition temperature of the sample and lower minimum air temperature, while the necessary time for ignition increased. The elapsed time was in the range of 3 to 30 min, i.e. comparable in order of magnitude to the forward-flow cases of the present study. Similar results were found by Ronda et al. [22] with pine bark in a forced flow reactor with the air flow heated up to 250 °C. An increased air flow rate cooled the sample and inhibited the reaction.

4.4. Forward and opposed smouldering propagation

Above, it was been found that a substantial rate of heat was lost during the experiments, both from the metal objects under the sample (Section 3.4.1) and by gas flows above it (Section 3.4.2). Uneven thermal development, with horizontal and vertical temperature differences (Section 3.3.2) contributed to driving forces for air flows inside the sample. Uprising buoyant flows gave downward flows in other parts of the sample (Section 4.2). For the opposed-flow configuration, i.e., without air draft inlet from below, these circulating motions were the only supply of air. In the forward-flow cases, an air flow was introduced into the bottom of the sample (Section 2.3). Although it was found to have a limited flowrate (Section 3.4.2), the difference made was apparent and significant.

It was deduced that fresh air was brought down into the cavity of the steel pipe, above the sample, and further down into the sample. Also for the forward-flow configuration, the airflow from above was considerably larger than the air supplied from below.

In summary, the smouldering propagation in the sample was partly supplied by oxygen from below, but mainly from above. Locations of forward smouldering and locations of opposed smouldering existed at the same time within the sample. Accordingly, the purely forward and purely opposed smouldering propagation were not obtained. This differs from slender systems like a narrow tube or cigarette, whereas it resembles practical cases like a pellets storage bin. This means that the terms “semi-forward” and “semi-opposed” could be more precise labels for the cases studied. On the other hand, even a modest additional airflow, as in the presented forward cases, had considerable impact on the behaviour. As seen in the results section, temperatures became higher and the consumption faster and more complete.

4.5. Flaming or non-flaming combustion

Obviously, Case VF3 developed into flaming combustion for a few minutes (Section 3.2.5). This was evident from the high temperatures (Table 2) in the sample and, in particular, above. In addition, the damages to the equipment left no doubt. The relevant issue was whether any other cases had flaming combustion. We did neither record the experiment on video, nor did we visually observe it continuously. However, the instances actually observed visually revealed no evidence of flaming. Some of the thermocouples recorded peak temperatures at a level that might indicate some flaming. For instance, in Case VF5 (Fig. 8), which had the highest temperatures besides case VF3, the temperatures at 6 and 8 cm height peaked to 781 °C and 801 °C, respectively, in Stage III. The simultaneous readings for the thermocouples straight above these (10–14 cm) were 160–380 degrees lower, which indicated that there were no uprising tongues of flame. Furthermore, even the most intensive combustion period (Stage III) had a duration of hours, while in flaming combustion, the same amount had been consumed in minutes (cf. Section 3.4.1). It can be remarked that the high temperatures were seen in the upper part of the sample, close to the open surface. On the other hand, it was noticed that the temperatures developed as a hot spot starting a 2–4 cm and moving upwards, cf. Fig. 8.

An issue here can be the definition of flaming versus smouldering. The distinction often found in literature must be understood as a reference to visible flame or not. However, visibility is troublesome to apply as a criterion. The discussion of Rein [3] pointed towards a criterion related to which reactions that are involved. Others have pointed at the presence of CO [56].

In Section 3.4.3, it was found that if CO, CH_4 and H_2 from pyrolysis rose to the sample surface, they would oxidize almost completely within the available timescales. That is, quite fast in the perspective of smouldering. Furthermore, it must be expected that the air motion into and within the pellets void were unevenly distributed. This means that some locations from time to time experienced a surplus of oxygen. Hence, there were possibilities of both gas-phase reactions of pyrolysates and of char oxidation within the pellets sample. Smouldering is often modelled by a 3–5 step reaction mechanism, including the oxidation of solid components like char. Such a set of global reactions emulates thousands of elementary reactions [57,58], where the great majority are gas-gas reactions. Accordingly, the distinction between smouldering and flaming as gas-solid vs. gas-gas reactions is not a clear criterion.

Basically, we have regarded the cases other than VF3 as primarily smouldering combustion, although incidental major gas-phase reactions can have occurred. The long process time, together with the lack of direct evidence of flames, were reasons for this viewpoint.

4.6. Practical considerations

The wide usage of wood pellets means that some results can have direct, everyday relevance. One of the most interesting result may be the fact that Type 1 forward smouldering was observed to take place: a lurking fire waiting for hours at low intensity before escalating.

One finding from the experiments was that the air supply is very important for the development of smouldering and flaming, and that a relatively small flow can make notable difference. For a storage bin or silo, it may seem obvious that direct air supply through openings must be avoided or carefully controlled. However, also the upper free surface of the stored body of pellets can receive air. The results here indicate that this surface should have a restriction or cover, to obstruct the air downdraft into it. It could, for instance, be some sort of a solid (and non-flammable) loose lid, moving with the surface as this is lowered during the gradual drain of the container.

5. Conclusions

Samples of 1.7 l of dry wood pellets (8 mm diameter) were tested in a set-up with intial heating from below. Configurations with and without draft-air inflow from below were tried to provide smouldering propagation. Time series of distributed temperature data were recorded, together with values of the sample mass.

The experiments with an air inlet was observed with two distinct smouldering behaviours: Type 1, where the sample after the period of external heating (6 h) cooled for 6–10 h, and then increased in temperature to intense smouldering, and Type 2, where the sample went into intense smouldering before the end of external heating. One of the latter cases developed into flaming combustion. In experiments without air draft, the sample cooled after external heating, before developing into intense smouldering about 20 h later.

The process could be divided into four main stages: Stage I with external heating, Stage II characterized by a moderate smouldering and partial cooling, Stage III with intense combustion, and the final Stage IV. All four periods were distinct for Type 1 draft flow and no-draft modes, while for Type 2 propagation, Stage III overlapped the external heating and no Stage II was observed.

Smouldering without air-draft inlet reached a maximum temperature of 550–635 °C after approximately 27 h, while draft-flow Type 1 reached 600–670 °C after 18 h and Type 2 reached 720–800 °C after 5 h. The total mass loss was approximately 90% with air-inlet cases, while approx. 85% for no-inlet cases. Propagation with air inflow was considerably faster than without, however, much slower than ordinary combustion for energy conversion.

All cases but one were regarded as predominantly smouldering combustion, in spite of relatively high peak temperatures. The discussion pointed out that criteria for distinguishing flaming and smouldering combustion are not clear.

The size of the sample was sufficiently large (diameter 0.15 m) to allow an uneven thermal development. It was found that buoyant flows in the pellets void caused downdraft of air into the sample from above, for both configurations. Consequently, there were possibilities for local excess of air, which could have caused temporarily high temperatures.

Differences in temperature gradient (heating rate) and temperature level were noted, which can contribute to explaining the development into non-sustained smouldering, delayed onset of smouldering after hours of cooling, and direct transfer to intense smouldering. However, more data are needed in this respect.

The difference between the two configurations was buoyant draft inflow of air into the bottom of the sample. Although modest, this inflow caused a substantial rise in smouldering and shortening of the elapsed time.

Fronts of drying and pyrolysis were identified and tracked. In addition, a front of oxidation was found in a part of all samples. However, some cases indicated that oxidation in wood pellets can propagate as a distributed reaction rather than a front.

CRediT authorship contribution statement

Virginia Rebaque: Conceptualization, Investigation, Methodology, Supervision, Visualization, Writing - review & editing. **Ivar S. Ertesvåg:** Conceptualization, Investigation, Methodology, Supervision, Visualization, Writing - review & editing. **Ragni Fjellgaard Mikalsen:** Investigation, Methodology, Conceptualization. **Anne Steen-Hansen:** Investigation, Methodology, Conceptualization.

Declaration of Competing Interest

The authors declare that they have no known competing financial interests or personal relationships that could have appeared to influence the work reported in this paper.

Acknowledgement

Analysis of the fuel was provided by the group of Professor Ulrich Krause at the Department of Process Safety and Environmental Engineering at Otto von Guericke University Magdeburg, Germany.

Funding: The first author conducted the work as an Erasmus exchange student from the Technical University of Madrid, Spain. The third author was funded by the Research Council of Norway, Project No. 238329: Emerging Risks from Smoldering Fires (EMRIS).

References

[1] Rein Guillermo. Smouldering combustion phenomena in science and technology. Int Rev Chem Eng 2009;1:3–18.
[2] Ohlemiller TJ. Modeling of smoldering combustion propagation. Prog Energy Combust Sci 1985;11(4):277–310. https://doi.org/10.1016/0360-1285(85)90004-8.
[3] Rein Guillermo, et al. Smoldering combustion. In: Hurley MJ, editor. SFPE Handbook of fire protection engineering 5th ed.New York: Springer; 2016. p. 581–603. https://doi.org/10.1007/978-1-4939-2565-0-19. ISBN 978-1-4939-2565-0.
[4] Ohlemiller TJ, et al. Smoldering combustion. In: DiNenno PJ, editor. SFPE handbook of fire protection engineering. 3rd ed.Quincy, MA: NFPA; 2002. p. 200–9. ISBN 0877654514.
[5] Palmer KN. Smouldering combustion in dusts and fibrous materials. Combust Flame 1957;1(2):129–54. https://doi.org/10.1016/0010-2180(57)90041-X.
[6] Torero JL, Fernandez-Pello AC. Natural convection smolder of polyurethane foam, upward propagation. Fire Saf J 1995;24(1):35–52. https://doi.org/10.1016/0379-7112(94)00030-J.
[7] Walter DC, Anthenien RA, Fernandez-Pello AC. Smolder ignition of polyurethane foam: effect of oxygen concentration. Fire Saf J 2000;34:343–59. https://doi.org/10.1016/S0379-7112(00)00007-2.
[8] Bar-Ilan A, Rein G, Fernandez-Pello AC, Torero JL, Urban DL. Forced forward smoldering experiments in microgravity. Exp Therm Fluid Sci 2004;28(7):743–51. https://doi.org/10.1016/j.expthermflusci.2003.12.012.
[9] Bar-Ilan A, Rein G, Walther DC, Fernandez-Pello AC, Torero JL, Urban DL. The effect of buoyancy on opposed smoldering. Combust Sci Technol 2004;176(12):2027–55. https://doi.org/10.1080/00102200490514822.
[10] Ohlemiller TJ. Smouldering combustion propagation on solid wood. Fire Safety Science – 3rd Int. Symp. 1991. p. 565–74. https://doi.org/10.3801/IAFSS.FSS.3-565. Edinburgh, Scotland.
[11] Carvalho Elaine R, Gurgel Veras Carlos A, Carvalho Jr. João A. Experimental investigation of smouldering in biomass. Biomass Bioenergy 2002;22(4):283–94. https://doi.org/10.1016/S0961-9534(02)00005-3.
[12] Huang Xinyan, Rein Guillermo. Downward and upward spread of smoldering peat fire. 10th U.S. National Combustion Meeting, April 23–26 2017. College Park, MD, USA: Organized by the Eastern States Section of the Combustion Institute; 2017. p. 1595–600. URL:http://toc.proceedings.com/34904webtoc.pdf. ISBN 978-1-5108-4238-0.
[13] Huang Xinyan, Restuccia Francesco, Gramola Michela, Rein Guillermo. Experimental study of the formation and collapse of an overhang in the lateral spread of smouldering peat fires. Combust Flame June 2016;168:393–402. https://doi.org/10.1016/j.combustflame.2016.01.017.
[14] Hadden Rory M, Rein Guillermo, Belcher Claire M. Study of the competing chemical reactions in the initiation and spread of smouldering combustion in peat. Proc Combust Inst 2013;34(2):2547–53. https://doi.org/10.1016/j.proci.2012.05.060.
[15] He Fang, Yi Weiming, Li Yongjun, Zha Jianwen, Luo Bin. Effects of fuel properties on the natural downward smoldering of piled biomass powder: experimental investigation. Biomass Bioenergy 2014;67:288–96. https://doi.org/10.1016/j.biombioe.2014.05.003.
[16] He Fang, Behrendt Frank. Experimental investigation of natural smoldering of char granules in a packed bed. Fire Saf J 2011;46(7):406–13. https://doi.org/10.1016/j.firesaf.2011.06.007.
[17] Krause Ulrich, Schmidt Martin. Propagation of smouldering in dust deposits caused by glowing nests or embedded hot bodies. J Loss Prev Process Ind 2000;13:319–26. https://doi.org/10.1016/S0950-4230(99)00031-5.
[18] Hagen Bjarne C, Frette Vidar, Kleppe Gisle, Arntzen Bjørn J. Onset of smoldering in cotton: effects of density. Fire Saf J 2011;46(3):73–80. https://doi.org/10.1016/j.firesaf.2010.09.001.
[19] Hagen Bjarne C, Frette Vidar, Kleppe Gisle, Arntzen Bjørn J. Effects of heat flux scenarios on smoldering in cotton. Fire Saf J 2013;61:144–59. https://doi.org/10.1016/j.firesaf.2013.08.001.
[20] Hagen Bjarne C, Frette Vidar, Kleppe Gisle, Arntzen Bjørn J. Transition from smoldering to flaming fire in short cotton samples with asymmetrical boundary conditions. Fire Saf J 2015;71:69–78. https://doi.org/10.1016/j.firesaf.2014.11.004.
[21] Fabris Ivo, Cormier Daniel, Gerhard Jason I, Bartczak Tomek, Kortschot Mark, Torero Jose L, Cheng Yu-Ling. Continous, self-sustaining smouldering destruction of simulated faeces. Fuel 2017;190:58–66. https://doi.org/10.1016/j.fuel.2016.11.014.
[22] Ronda A, Della Zassa M, Biasin A, Martin-Lara MA, Canu P. Experimental investigation on the smouldering of pine bark. Fuel 2017;193:81–94. https://doi.org/10.1016/j.fuel.2016.12.028.
[23] Fateev Vladimir, Agafontsev Mikhail, Volkov Sergey, Filkov Alexander. Determination of smoldering time and thermal characteristics of firebrands under laboratory conditions. Fire Saf J 2017;91:791–9. https://doi.org/10.1016/j.firesaf.2017.03.080.
[24] Steen-Hansen Anne, Mikalsen Ragni Fjellgaard, Jensen Ulla Eidissen. Smouldering combustion in loose-fill wood fibre thermal insulation. An experimental study. Fire Technol 2018;54(6):1–24. https://doi.org/10.1007/s10694-018-0757-4.
[25] Smucker Benjamin D, Mulky Tejas C, Cowan Daniel A, Niemeyer Kyle E, Blunck David L. Effects of fuel content and density on the smoldering characteristics of cellulose and hemicellulose. Proc Combust Inst 2019;37(3):4107–16. https://doi.org/10.1016/j.proci.2018.07.047.
[26] Dosanjh S, Peterson J, Fernandez-Pello AC, Pagni PJ. Buoyancy effects on smoldering combustion. Acta Astronaut 1986;13(11–12):689–96. https://doi.org/10.1016/0094-5765(86)90019-6.
[27] Torero JL, Fernandez-Pello AC. Forward smolder of polyurethane foam in a forced air flow. Combust Flame 1996;106(1–2):89–109. https://doi.org/10.1016/0010-2180(95)00245-6.
[28] Lutsenko Nickolay A, Levin Vladimir A. Effect of gravity field and pressure difference on heterogeneous combustion in porous media. Combust Sci Technol 2014;186(10–11):1410–21. https://doi.org/10.1080/00102202.2014.934611.
[29] Huang Xinyan, Rein Guillermo. Thermochemical conversion of biomass in smouldering combustion across scales: the roles of heterogeneous kinetics, oxygen and transport phenomena. Bioresour Technol 2016;207:409–21. https://doi.org/10.1016/j.biortech.2016.01.027.
[30] Ohlemiller TJ, Lucca DA. An experimental comparison of forward and reverse smolder propagation in permeable fuel beds. Combust Flame 1983;54(1–3):131–47. https://doi.org/10.1016/0010-2180(83)90027-5.
[31] Drysdale Dougal. An introduction to fire dynamics. 3rd ed. Chichester, UK: John Wiley & Sons978-0-470-31903-1; 2011.
[32] Ohlemiller Thomas J. Forced smolder propagation and the transition to flaming in cellulosic insulation. Combust Flame 1990;81:354–65. https://doi.org/10.1016/0010-2180(90)90031-L.
[33] Dodd Amanda B, Lautenberger Christopher, Fernandez-Pello Carlos. Computational modeling of smolder combustion and spontaneous transition to flaming. Combust Flame 2012;159(1):448–61. https://doi.org/10.1016/j.combustflame.2011.06.004.
[34] Gentilhomme Olivier, Truchot Benjamin, Verdier Florent, Poichotte François, Barrier-Guillot Bruno. Experimental investigation of a smouldering fire in an under-ventilated silo. Process Saf Prog (2), 2019.;38. https://doi.org/10.1002/prs.12012.
[35] Jensen Ulla E. The development of smouldering combustion in combustible building insulation materials [Master's thesis]. Trondheim, Norway: Department of Civil and Transport Engineering, NTNU Norwegian University of Science and Technology; 2016 URL:http://hdl.handle.net/11250/2385048 [accessed 19.06.2019].
[36] Mikalsen RF, Hagen BC, Steen-Hansen A, Frette V. Extinguishing smoldering fires in wood pellets through cooling. 5th Magdeburg Fire and Explosions Days 2017. Magdeburg, Germany: Otto-von-Guericke-University; 2017. https://doi.org/10.978.300/0562013.
[37] Mikalsen RF, Hagen BC, Frette V. Synchronized smoldering combustion. EPL 2018;121:5. https://doi.org/10.1209/0295-5075/121/50002.
[38] Mikalsen Ragni Fjellgaard, Hagen Bjarne Christian, Steen-Hansen Anne, Krause Ulrich, Frette Vidar. Extinguishing smoldering fires in wood pellets with water cooling: an experimental study. Fire Technol 2019;55(1):257–84. https://doi.org/10.1007/s10694-018-0789-9.
[39] Mikalsen RF. Fighting flameless fires – Initiating and extinguishing self-sustained smoldering fires in wood pellets [Doctoral thesis] Magdeburg, Germany: Otto von Guericke University Magdeburg; 2018 URL: http://www.diva-portal.org/smash/get/diva2:1251941/FULLTEXT01.pdf [accessed 19.06.2019].
[40] Rebaque Valdés V. Smouldering fires in wood pellets. Specialization project report. Department of Energy and Process Engineering, NTNU Norwegian University of Science and Technology; 2016.
[41] Rebaque Valdés V. Experimental study of smouldering fires in wood pellets [Master's thesis] Trondheim, Norway: Department of Energy and Process Engineering, NTNU Norwegian University of Science and Technology; 2017 URL: http://hdl.handle.net/11250/2454929 [accessed 19.06.2019].
[42] Larsson Ida, Lonnermark Anders, Blomqvist Per, Persson Henry, Bohlen Haleh. Development of a screening test based on isothermal calorimetry for determination of self-heating potential of biomass pellets. Fire Mater 2017;41(8):940–52. https://doi.org/10.1002/fam.2427.
[43] Guo Wendi, Trischuk Ken, Xiaotao Bi C, Lim Jim, Sokhansanj Shahab. Measurements of wood pellets self-heating kinetic parameters using isothermal calorimetry. Biomass Bioenergy 2014;63:1–9. https://doi.org/10.1016/j.biombioe.2014.02.022.
[44] McCaffrey BJ, Heskestad G. A robust bidirectional low-velocity probe for flame and fire application. Combust Flame 1976;26:125–7. https://doi.org/10.1016/0010-2180(76)90062-6.
[45] Kreith F, Bohn MS. Principles of heat transfer. 6th ed. Pacific Grove CA: Brooks/Cole0-314-01360-1; 2001.
[46] Gryzagoridis J. Natural convection from a vertical flat plate in the low Grashof number range. Int J Heat Mass Transfer 1971;14(1):162–5. https://doi.org/10.1016/0017-9310(71)90149-9.
[47] Thermostahl Romania. URL:www.thermostahl.ro [accessed 19.06.2019].
[48] Pelltech OÜ. URL:www.pelltech.eu [accessed 19.06.2019].
[49] Turns Stephen R. An introduction to combustion: concepts and applications. 3rd ed. McGraw-Hill; 2012.
[50] Westbrook Charles K, Dryer Frederick L. Simplified reaction mechanisms for the

oxidation of hydrocarbon fuels in flames. Combust Sci Technol 1981;27(1–2):31–43. https://doi.org/10.1080/00102208108946970.
[51] Fernandez-Anez Nieves, Kristensen Kim, Rein Guillermo. Two-dimensional model of smouldering combustion using multi-layer cellular automaton: the role of ignition location and direction of airflow. Fire Saf J 2017;91:243–51. https://doi.org/10.1016/j.firesaf.2017.03.009.
[52] Ertesvåg Ivar S. Turbulent flow and combustion (in Norwegian). Trondheim, Norway: Tapir Academic Publisher82-519-1568-6; 2000.
[53] Anca-Couce Andrés, Zobel Nico, Berger Anka, Behrendt Frank. Smouldering of pine wood: kinetics and reaction heats. Combust Flame 2012;159(4):1708–19. https://doi.org/10.1016/j.combustflame.2011.11.015.
[54] Kashiwagi Takashi, Nambu Hidesburo. Global kinetic constants for thermal oxidative degradation of a cellulosic paper. Combust Flame 1992;88(3–4):345–68. https://doi.org/10.1016/0010-2180(92)90039-R.
[55] van Blijderveen Maarten, Gucho Eyerusalem M, Bramer Eddy A, Brem Gerrit. Spontaneous ignition of wood, char and RDF in a lab scale packed bed. Fuel 2010;89(9):2393–404. https://doi.org/10.1016/j.fuel.2010.01.021.
[56] Andreae MO, Merlet P. Emission of trace gases and aerosols from biomass burning. Global Biogeochem Cycles 2001;15(4):955–66. https://doi.org/10.1029/2000GB001382.
[57] Németh András, Blazso Marianne, Baranyai Péter, Vidóczy Tamás. Thermal degradation of polyethylene modeled on tetracontane. J Anal Appl Pyrol 2008;81(2):237–42. https://doi.org/10.1016/j.jaap.2007.11.012.
[58] Gascoin N, Navarro-Rodriguez A, Fau G, Gillard P. Kinetic modelling of high density polyethylene pyrolysis: part 2. Reduction of exisiting detailed mechanism. Polym Degrad Stabil 2012;97(7):1142–50. https://doi.org/10.1016/j.polymdegradsTable2012.04.002.